



Open Chemistry Journal

Content list available at: <https://openchemistryjournal.com>



RESEARCH ARTICLE

Iron(II) Spin Crossover Polymers of Planar N₂O₂ Schiff Base Templates and 4,4'-bis(pyridyl)urea Bridges

Lisa Zappe¹, Charles Lochenie², Thomas Martin³ and Birgit Weber^{1,*}

¹Department of Chemistry, Inorganic Chemistry IV, University of Bayreuth, Bayreuth, Germany

²Institut de Science et d'Ingénierie Supramoléculaires, Strasbourg, France

³Department of Chemistry, Inorganic Chemistry I, University of Bayreuth, Bayreuth, Germany

Abstract:

Introduction:

The synthesis of four new iron(II) coordination polymers [Fe(L1a)(bpua)] (**1**), [Fe(L1b)(bpua)](0.5bpua) (**2**), [Fe(L2a)(bpua)] (**3**), [Fe(L1b)(bpua)](yEtOH) (**5**) and one trinuclear complex [$\{\text{Fe}(\text{L}1\text{a})(\text{bpua})(\text{MeOH})\}_2-\mu\{\text{Fe}(\text{L}1\text{a})\}(\text{xMeOH})$] (**4**) with Schiff base-like N₂O₂ coordinating equatorial ligands (L1a, L1b and L2a) and 4,4'-bis(pyridyl)urea (bpua) as bridging axial ligand is described.

Materials and Methods:

Single crystal X-ray structure elucidation of the trinuclear module **4** and of the coordination polymer **5** reveals the presence of HS-LS-HS chains and all-HS infinite 1-D strands, respectively. As anticipated the presence of the bridging urea supports the supramolecular concatenation within an extended hydrogen-bonding network. Magnetic measurements reveal spin crossover behavior for four of the five complexes (**1** – **4**) that is strongly solvent dependent.

Results and Conclusion:

Interestingly, in two cases, complete removal of the solvent from the crystal packing leads to wider thermal hysteresis loops.

Keywords: Iron, Schiff base ligand, Spin crossover, Hydrogen bonding, Polymers, Thermal hysteresis.

Article History

Received: March 06, 2018

Revised: May 17, 2018

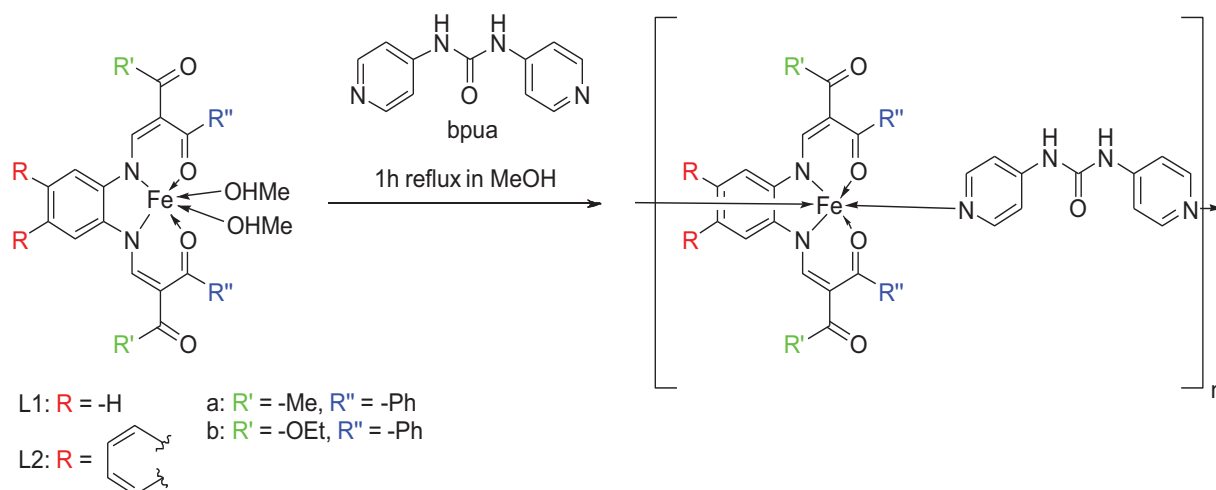
Accepted: February 21, 2019

1. INTRODUCTION

Molecules that can shuttle between two or more energetically close-lying geometrical and/or electronic states qualify as sensor and actor materials. Being responsive to changes in environmental conditions or external stimuli, such molecular switches can undergo discrete stereo-electronic transitions among these states which, importantly, may be controlled by some operator. For this reason, switchable molecules attract ongoing interest of scientists from very interdisciplinary fields due to their application potential as molecular sensor and actors or for data storage at the molecular level [1 - 4]. Along the latter line of research, Spin Crossover (SCO) complexes are prominent protagonists as they undergo stimulated transitions (thermal agitation or irradiation of light, etc.) between discrete magnetic states with similarly discrete

optical properties. As inherently the largest divergence in the material's read-out properties accompanies the largest aspect of the spin states' magnetic properties, the majority of the spin crossover complexes investigated so far relies on the non-toxic and very abundant iron(II) as metal center [5 - 7]. The predominance of iron(II) can thus be traced to the switching between a paramagnetic $S = 2$ High Spin (HS) state and a diamagnetic $S = 0$ Low Spin (LS) state which massively alters the population of anti-bonding e_g -type orbitals and, through this, strongly affects the metal-ligand bond lengths. This effect on the inner coordination sphere with all of its stereochemical and elec-tronic consequences can be triggered by a wide range of different physical or chemical stimuli, e.g. change in temperature [8], pressure [9], pH [10], or light irradiation [11]. In some cases, the combination of different stimuli leads to unexpected behavior, as for example a pressure-induced spin-crossover photomagnet [12]. Whereas SCO inherently is a molecular phenomenon, its amplification *via* supramolecular concatenation may give rise to the emergence of higher-order

* Address correspondence to this author at the Department of Chemistry, Inorganic Chemistry II, University of Bayreuth, Bayreuth, Germany; Tel: +49 921 552555; Fax: +49 921 552157; E-mail: weber@uni-bayreuth.de



Scheme 1. General procedure for the synthesis of the iron(II) coordination polymers [Fe(L1a)(bpua)] (1), [Fe(L1b)(bpua)](0.5bpua) (2), and [Fe(L2a)(bpua)] (3) and used abbreviations.

effects. For instance, a given system made of SCO-active units may express either of two macroscopically different magnetic states at the same temperature dependent on the history of the system [5, 13 - 21]. The underlying chemical forces which translate cooperativity among neighboring molecular units into magnetic bistability of the material are not known in detail in many of the reported cases.

A highly interesting aspect of SCO materials is that the spin state change can be combined with additional functionalities yielding multifunctional materials where synergetic effects between the different functions are possible [13, 17]. The combination of the SCO phenomenon with additional properties such as liquid crystal/phase transition behavior [22 - 32], magnetic exchange interactions [33], or photoluminescence [34 - 38] can be realized through modification of the ligand. This is highly relevant for potential applications, as either additional read-out possibilities are realized (*e.g.* change in luminescence) or new ways to trigger the spin state switch (*e.g.* phase transition) are established. Multiple functionalities can also be implemented through the combination of a cationic SCO complex with a functional counter ion (*e.g.* electrical conductivity [39 - 41] or ferromagnetism [42]). Nano-sized SCO complexes are highly relevant for future applications and offer further pathways towards multifunctional systems *e.g.* through surface modification or to fine-tune the SCO properties. [43 - 47]

For all those multifunctional or nano-sized examples, high cooperativity leading to the observation of wide hysteresis loops is highly desirable. This is important for the application in the field of sensors with memory effect or data storage. There is growing evidence for supramolecular networks of hydrogen bridges being a preferential requisite of cooperativity in the solid state [48]. Accordingly, there is a continuous need for new spin crossover systems that harness hydrogen-bond networks to impose new or improved SCO properties or new functionalities. Inspired by the results with *N*-(pyrid-4-yl)isonicotinamide as bridging axial ligand, that yielded very wide (up to 88 K) and stable thermal hysteresis loops around

room temperature [49], in the present study 4,4'-bipyridylurea (bpua) is used. We introduced bis-pyridine substituted urea moieties as N-ligating and potentially bridging ligands to our Schiff-base based square-planar templating tetradentate N₂O₂ ligand platform in iron(II) complexes [50 - 54]. These axial ligands combine a moderate to strong ligand field with an almost linear directionality about the binding sites, implying minor steric stress in coordination polymers. Additionally, the ligand field strength of bpua can be influenced by the addition of molecules that interact with the protons of the urea moiety [55]. It was demonstrated already that the energy of the hydrogen atoms in bpua can be changed by the addition of counter ions [55]. In addition, the urea moiety is well known to support multiple hydrogen-bonding interactions, both as a donor and an acceptor. Herein we have combined this symmetric and rigid linker with several N₂O₂ derivatives L1a/b and L2a/b and have studied the solid state structures and magnetic response through X-ray crystallography (single crystals and powder diffraction) and SQUID magnetometry.

2. MATERIALS AND METHODS

The used solvents Methanol (MeOH) and Ethanol (EtOH) were purified as described in the literature [56]. The starting iron(II) complexes [Fe(L1a)(MeOH)₂], [Fe(L1b)(MeOH)₂] and [Fe(L2a)(MeOH)₂] were synthesized as described previously [57 - 59] with iron(II) acetate [60] as iron source. Bpua was synthesized as described in the literature [55]. The starting materials were used without further purification. All iron(II) complexes were synthesized under inert conditions (argon 5.0) using Schlenk techniques.

CHN analyses were measured with a Vario El III from Elementar Analysen-Systeme. Mass spectra were recorded with a Finnigan MAT 8500 with a data system MASPEC II. Magnetic susceptibility data were collected using a MPMSXL-5 SQUID magnetometer under an applied field of 0.5 T over the temperature range 10 to 400 K in the sweep mode (5K/min). The samples were placed in gelatin capsules held within a plastic straw. The data were corrected for the dia-

magnetic contributions of the ligands by using tabulated Pascal's constants [61] and of the sample holder. Powder diffractograms were measured with a *STOE StadiP* diffractometer using $\text{CuK}_{\alpha 1}$ radiation with a Ge monochromator, and a Mythen 1K Stripdetector in transmission geometry.

The diffraction data of **4** and **5** were collected with a *STOE StadiVari* diffractometer using graphite-monochromated MoK_{α} radiation. The data were corrected for Lorentz and polarization effects. The structure was solved by direct methods (SIR-97 (SIR-97) [62 - 64] and refined by full-matrix least-square techniques against $\text{Fo}^2\text{-Fc}^2$ (SHELXL-97) [65] using WinGX [66]. All hydrogen atoms were calculated in idealized positions with fixed displacement parameters. ORTEP-III [67, 68] was used for the structure representation, Mercury [69] to illustrate the crystal packing. Cif files were deposited at the CCDC database (**4**: CCDC 1827146; **5**: CCDC 1827147).

3. EXPERIMENTAL

Synthesis of $[\text{Fe}(\text{L1a})(\text{bpua})]$ (**1**): 0.2 g (0.35 mmol) $[\text{Fe}(\text{L1a})(\text{MeOH})_2]$ and 0.22 g (1.05 mmol) bpua were dissolved in 20 mL MeOH and refluxed for 1 hour. In the dark red solution, a fine crystalline black precipitate was obtained overnight, that was filtered off, washed two times with 2 mL MeOH and dried in vacuum. Yield: 0.20 g (80%). MS (70eV), *m/z* (%): 506 $[\text{FeL1a}^+]$, 214 (bpua^+); elemental analysis (%) calcd. for $\text{C}_{39}\text{H}_{32}\text{FeN}_6\text{O}_5$ (720.57): C 65.01, H 4.48, N 11.66; found: C 65.20, H 4.33, N 11.52; IR: $\nu = 1760(\text{s})$ (CO bpua), $1589(\text{s})$ (CO) cm^{-1} .

Synthesis of $[\text{Fe}(\text{L1b})(\text{bpua})](0.5\text{bpua})$ (**2**): 0.2 g (0.317 mmol) $[\text{Fe}(\text{L1b})(\text{MeOH})_2]$ and 0.2 g (0.951 mmol) bpua were dissolved in 20 mL EtOH and refluxed for 1 hour. In the brown solution a black-greenish fine crystalline powder precipitated, that was filtered off, washed two times with 2 mL EtOH and dried in vacuum. Yield: 0.21 mg (75%). MS (FAB(+), 70eV), *m/z* (%): 566 $[\text{FeL1b}^+]$, 214 (bpua^+); elemental analysis (%) calcd. for $\text{C}_{46.5}\text{H}_{41}\text{FeN}_8\text{O}_{7.5}$ (887.74): C 62.91, H 4.66, N 12.62; found: C 62.91, H 4.65, N 12.65; IR: $\nu = 1762(\text{s})$ (CO bpua), $1625(\text{s})$ (CO), $1587(\text{s})$ (CO) cm^{-1} .

Synthesis of $[\text{Fe}(\text{L2a})(\text{bpua})]$ (**3**): 0.5 g (0.91 mmol) $[\text{Fe}(\text{L2a})(\text{MeOH})_2]$ and 0.62 g (2.90 mmol) bpua were dissolved in 100 mL MeOH and refluxed for 15 minutes. A brown fine crystalline powder precipitated, that was filtered off, washed with 20 mL MeOH and dried in vacuum. Yield: 0.59 g (85%). MS (70eV), *m/z* (%): 556 $[\text{FeL2a}^+]$, 214 (bpua^+); elemental analysis calcd (%) for $\text{C}_{43}\text{H}_{34}\text{FeN}_6\text{O}_5$ (770.63): C 67.02, H 4.45, N 10.91; found: C 67.52, H 4.35, N 10.80; IR: $\nu = 1755(\text{s})$ (CO bpua), $1592(\text{s})$ (CO) cm^{-1} . Please note, the carbon value obtained in the CHN analysis is too low due to incomplete combustion. The same difficulties were encountered for similar complexes of this ligand type with extended aromatic units [35, 51, 57, 70].

In order to receive single crystals of the coordination polymers **1** – **3** a diffusion setup was used employing a Schlenk tube separated in two parts with a glass wall. The starting iron(II) complex was placed on one side and the bridging ligand bpua on the other side of the glass wall and both parts were filled up with the solvent (MeOH or EtOH) to enable

diffusion between the two chambers. This setup was left standing at room temperature for several weeks. By this, single crystals were grown of a trinuclear complex with the composition $[\{\text{Fe}(\text{L1a})(\mu\text{-bpua})(\text{MeOH})\}_2\{\text{Fe}(\text{L1a})\}](8\text{MeOH})$ (**4**) and the coordination polymer $[\text{Fe}(\text{L1b})(\text{bpua})](2\text{EtOH})$ (**5**). In both cases, only few single crystals were obtained that allowed the determination of the X-ray structure and magnetic measurements but no further characterization of the material. Thus there are no results from elemental analysis and powder X-ray diffraction. The difference in the reaction conditions (room temperature vs. boiling point of the solvent) is most likely the reason for the different composition of the products.

4. RESULTS AND DISCUSSION

4.1. Synthesis and General Characterization

Given in Scheme. 1 is the general pathway for the synthesis of the coordination polymers $[\text{Fe}(\text{Lxy})(\text{bpua})]_n$ (**1** – **3**) and the used abbreviations. The bulk synthesis approach (mixing of the starting materials in a suitable solvent and heating to reflux) yielded the desired products as fine crystalline powders in good yield. In the case of $[\text{Fe}(\text{L1a})(\text{bpua})]$ (**1**) and $[\text{Fe}(\text{L2a})(\text{bpua})]$ (**3**) no solvent is included according to elemental analysis, whereas in the case of $[\text{Fe}(\text{L1b})(\text{bpua})](0.5\text{bpua})$ (**2**) satisfactory elemental analysis results were obtained by assuming that half an additional molecule of bpua is included. The obtained coordination polymers were characterized using elemental analysis, mass spectrometry, IR spectroscopy and powder X-ray diffraction. Diffusion setups were used to grow single crystals of the complexes, however, as illustrated below, a different composition is obtained for the single crystals compared to the bulk material. A trinuclear complex with the composition $[\{\text{Fe}(\text{L1a})(\mu\text{-bpua})(\text{MeOH})\}_2\{\text{Fe}(\text{L1a})\}](8\text{MeOH})$ (**4**) is obtained from the diffusion setup with $[\text{Fe}(\text{L1a})(\text{MeOH})_2]$ as starting material, whereas the coordination polymer $[\text{Fe}(\text{L1b})(\text{bpua})](2\text{EtOH})$ (**5**) crystallized without of additional bpua in the crystal packing.

4.2. X-ray Structure Analysis

In Fig. (1) an ORTEP drawing of the asymmetric unit of the two complexes **4** and **5** is given. **4** crystallizes in the triclinic space group P-1 with 2 molecules in the unit cell. **5** crystallizes in the monoclinic space group $\text{P}2_1/\text{c}$ with 4 molecules in the unit cell. Selected bond lengths and angles are summarized in Table 1. An overview of crystallographic data is given in Table S1.

The trinuclear complex **4** consists of three $[\text{Fe}(\text{L1a})]$ -units that are connected through two bpua ligands. Consequently the iron(II) centre in the middle (Fe2) has an N_4O_2 coordination sphere with two bpua as axial ligands, whereas the two outer iron centres (Fe1 and Fe3) have an N_3O_3 coordination sphere with one methanol molecule in each case as the sixth ligand. As expected, the O1–Fe1–O2 and the O12–Fe3–O13 angles of 106° and 107° , respectively, are in the region typical for high spin iron(II). This is in agreement with previous results on similar complexes of this ligand type with an N_3O_3 coordination sphere [71]. The O7–Fe2–O8 angle of 88° is in the

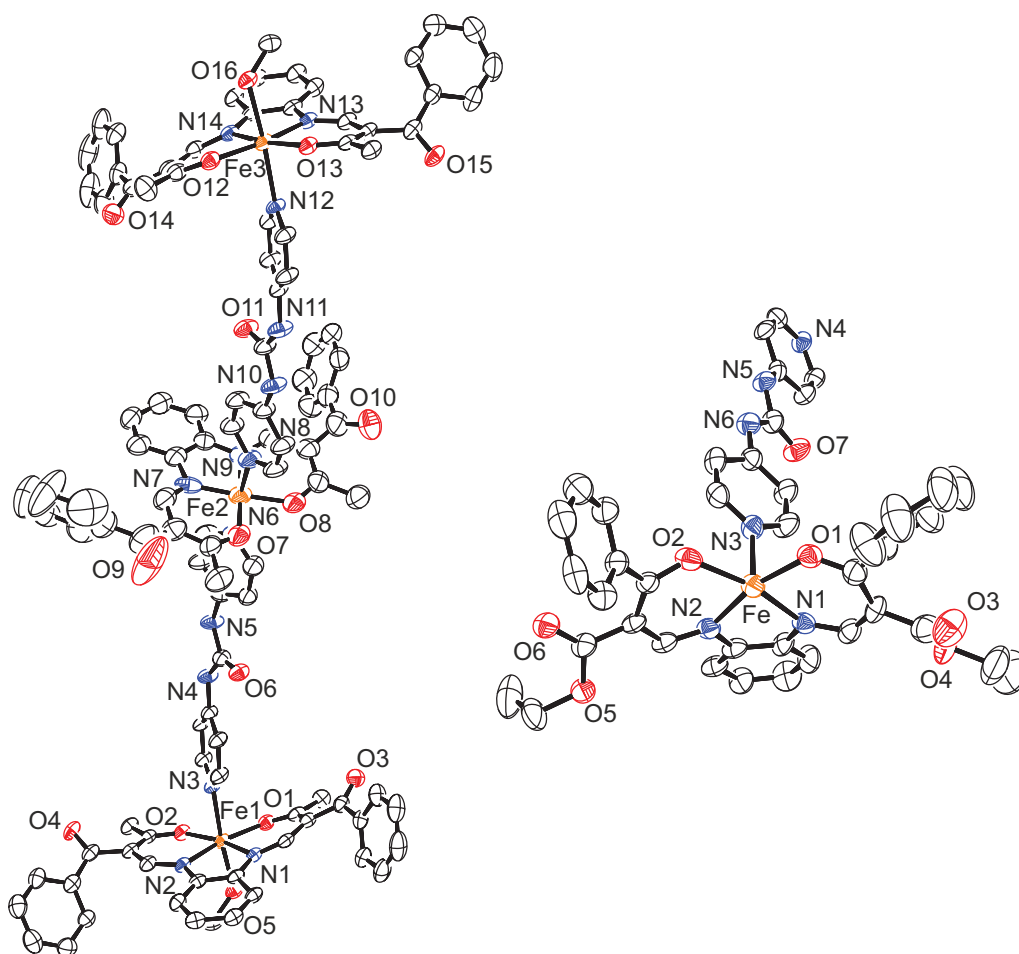


Fig. (1). ORTEP drawing of the asymmetric units of the trinuclear molecule **4** (left) and the polymeric complex **5** (right) and used atom numbering scheme.

Table 1. Selected bond lengths/Å, and angles/° within the inner coordination sphere of the iron(II) complexes discussed in this work. Crystal data determined at 133 K.

	Fe–N _{eq}	Fe–O _{eq}	Fe–N/O _{ax}	O _{eq} –Fe–O _{eq}	N _{ax} –Fe–N/O _{ax}
4/Fe1	2.071(3) 2.077(3)	2.016(3) 2.017(2)	2.235(3) 2.221(2)	106.10(10)	172.33(10)
Fe2	1.863(5) 1.903(4)	1.918(4) 1.933(4)	2.001(3) 2.002(4)	88.52(16)	173.85(15)
Fe3	2.074(3) 2.091(3)	2.020(2) 2.021(3)	2.224(3) 2.204(3)	107.85(10)	173.27(10)
5	2.041(7) 2.072(7)	2.001(6) 2.011(6)	2.179(6) 2.202(6)	107.6(2)	175.1(3)

region typical for low spin iron(II) complexes in this ligand systems [72 - 76]. The Fe–L bond lengths around the first coordination sphere of the iron centres, given in Table 1, are in line with a LS state for the N₄O₂-coordinated Fe2 and a HS state for Fe1 and Fe3.

In the case of **5**, one iron(II) center per asymmetric unit is observed. It has an octahedral N₄O₂ coordination sphere consisting of the equatorial tetradentate Schiff base-like ligand

L1b and the bridging axial ligand bpua. The O1–Fe1–O2 angle is 107.65° and therefore typical for iron(II) HS complexes of this ligand type [72 - 76]. The Fe–L bond lengths within the first coordination sphere confirm this spin state. As illustrated in Fig. (2), the polymer chains are almost perfectly linear due to the rigid nature of the bridging bpua ligand. Only a slight bending between neighbouring planes of the equatorial ligand is observed with an angle of 31° (see Figure S1). Adjacent polymer chains are connected to each other along the b-axis *via*

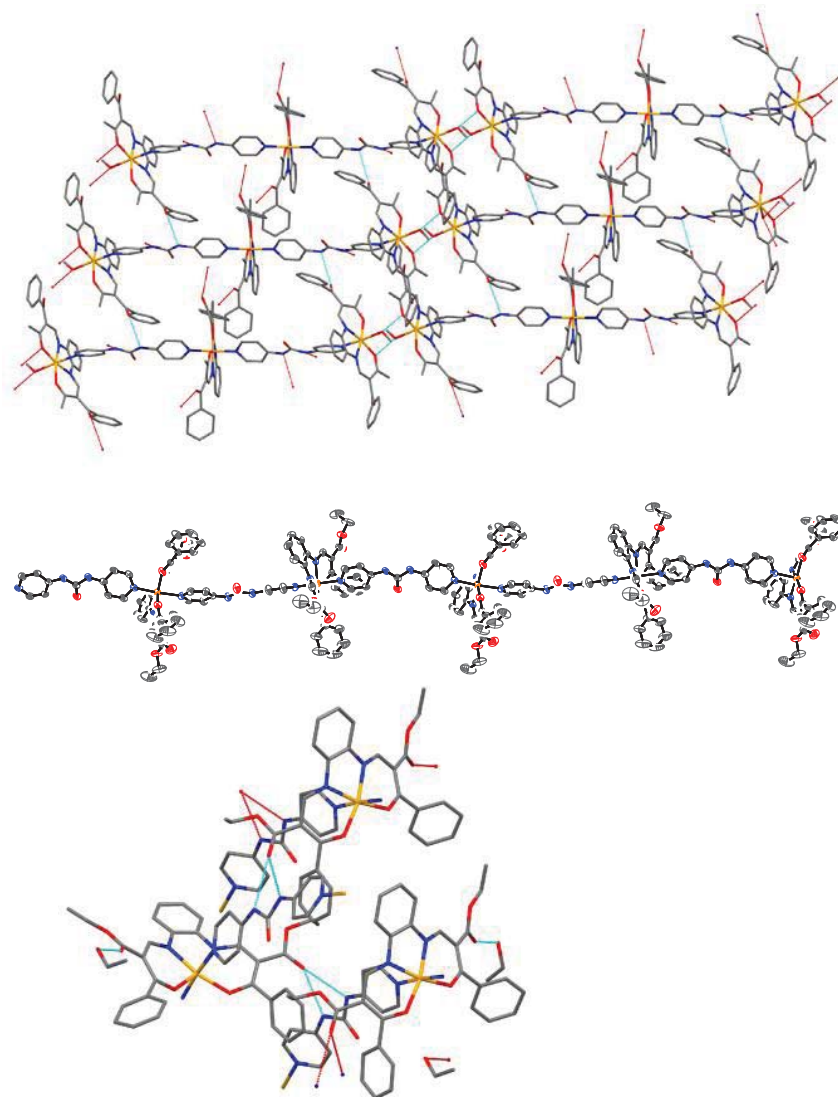


Fig. (2). Top: Packing of the trinuclear complex **4** illustrating the hydrogen bond network discussed in the manuscript. Middle: ORTEP drawing of a 1D chain of **5** and Bottom: excerpt of the packing of the polymeric complex **5** to illustrate the hydrogen bond network discussed in the manuscript.

hydrogen bonds $O5 \cdots H5A-N5$ with a distance of 2.111 Å and $O5 \cdots H6A-N6$ with a distance of 1.979 Å. A further contact to solvent molecules is observed between $O3 \cdots H51-O51$ with a distance of 2.156 Å.

The packing of the molecules of **4** in the crystal is displayed at the top of Fig. (2). The trinuclear molecules of **4** are stacked with an offset of the half length of the axial ligand to each other *via* hydrogen bonds from H4(N4) and H5(N5) of bpua *via* Methanol O201-H201 to O10 of the equatorial ligand. Thus, the offset of the trinuclear molecules can be explained by the formation of an infinite hydrogen bond network that interconnects the individual trinuclear molecules among each other. This network is spread in three directions. Along the a-axis, the trinuclear molecules are connected *via* the bpua N10-H10A to the equatorial ligand O15 with a distance of 2.458 Å and from N5-H5 of bpua to O3 of the equatorial ligand with a distance of 2.503 Å. The second connection along the bc-plane is made up by bpua N4-H4 *via* methanol O201-H201 (2.007 Å) to O10

(1.907 Å) of the equatorial ligand. Along the c-axis the endgroups are connected with each other *via* O5H5 to O12 (2.097 Å) and O16H16 to O2 (2.015 Å). As anticipated, the bpua ligand shows a high tendency for the formation of hydrogen bond networks.

In the Supporting Information, Figure S2, the calculated powder X-ray diffraction pattern of **4** and **5** is compared with that of the corresponding bulk complexes **1** and **2**, respectively. In both cases, no similarities are observed. This is not surprising due to the differences in the composition, but also due to the strong impact of the hydrogen bond network on the crystal packing.

4.3. Magnetic Properties

Temperature dependent measurements of the magnetic susceptibility were performed for all five samples using a SQUID magnetometer. The results are presented as a plot of the molar magnetic susceptibility (χ_M) temperature (T) product

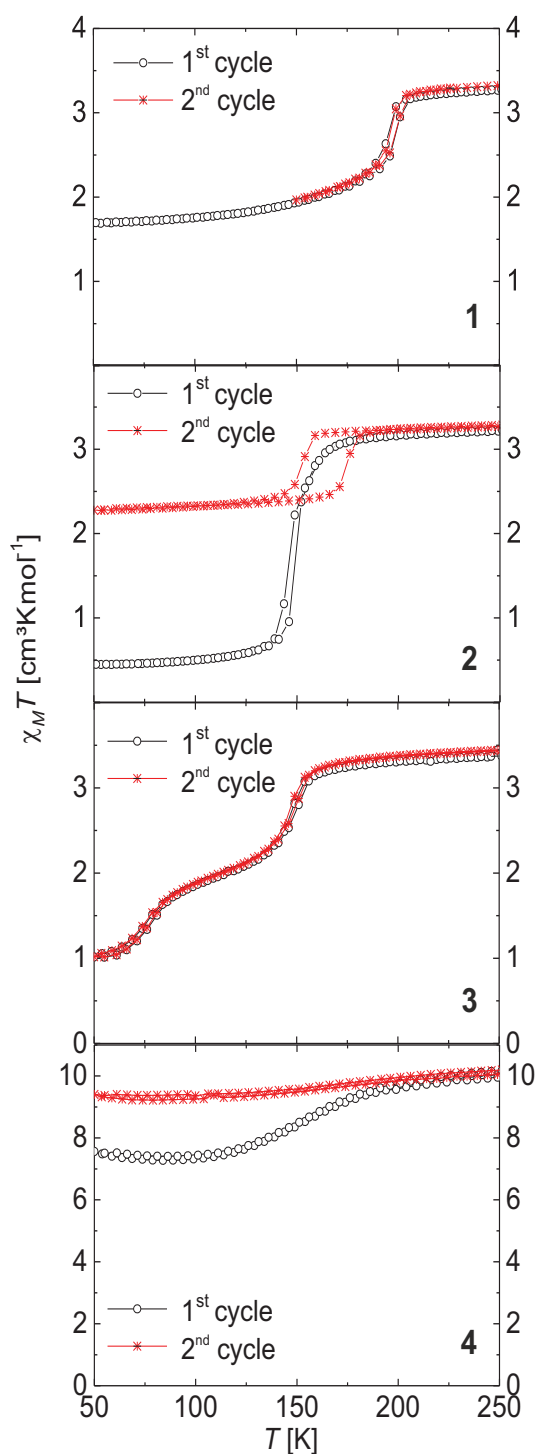


Fig. (3). Plot of the $\chi_M T$ product vs. T in the 250 – 50 K range for the complexes **1** – **4** discussed in this manuscript. Prior to the second cycle the sample was heated to 400 K.

versus T for samples **1** – **4** in Fig. (3) in the 50 – 250 K temperature region. The results of **5** and not completely dried powder samples of **1** (**1***) are given in the Supporting Information, Figure S3.

4.3.1. Coordination Polymers

At room temperature, for all coordination polymers a $\chi_M T$ product in the region of 3.1 – 3.4 cm³ K mol⁻¹ per iron center is obtained that is typical for iron(II) in the HS state. Upon cooling, the $\chi_M T$ product does not change with temperature for **5**, in agreement with the results from single crystal XRD (HS at 133 K). Thus **5** is a pure HS complex. All other samples show different types of SCO in the temperature range between 200 K and 100 K.

In the case of **1** an incomplete Spin Transition (ST) with $T_{1/2\downarrow} = 196$ K and $T_{1/2\uparrow} = 199$ K is observed, revealing a 3 K wide thermal hysteresis loop. At 100 K the $\chi_M T$ product of 1.76 cm³ K mol⁻¹ is in the region expected for a mixture of LS and HS states. Such a behavior is very frequently observed for coordination polymers of this ligand type [75, 77]. If the measurements are performed on a not completely dried sample (see SI, Figure S3), initially an incomplete gradual SCO is observed and the hysteresis appears after heating to 400 K. For the completely dried sample the SCO behavior does not change upon heating to 400 K in line with the results of elemental analysis that indicates the absence of solvent molecules.

In the first cooling/heating cycle **2** shows an almost complete ST with $T_{1/2\downarrow} = 145$ K and $T_{1/2\uparrow} = 149$ K (4 K hysteresis) and a $\chi_M T$ product of 0.46 cm³ K mol⁻¹ at 100 K. After annealing at 400 K, the ST is shifted to slightly higher temperatures ($T_{1/2\downarrow} = 152$ K and $T_{1/2\uparrow} = 174$ K) with a significantly broadened hysteresis loop (22 K) and a less complete ST with a $\chi_M T$ product of 2.34 cm³ K mol⁻¹ at 100 K.

In the case of **3** an incomplete two-step SCO is observed with $T_{1/2,1} = 149$ K and $T_{1/2,2} = 75$ K. At 125 K the $\chi_M T$ product is 2.07 cm³ K mol⁻¹ and at 50 K the $\chi_M T$ product is 0.99 cm³ K mol⁻¹. As for **1**, elemental analysis indicates the absence of solvent molecules and the SCO behavior does not change upon heating to 400 K.

Powder XRD patterns were recorded for the powder samples **1** – **3** at room temperature and 125 K to analyze whether the spin state change is accompanied by a phase transition. The results are displayed in Fig. (4). In all three cases, changes in the PXRD pattern are observed upon the spin transition. However, most of the patterns are only shifted thus the changes are most likely due to the change in the bond lengths and not due to a supplementary phase transition.

4.3.2. Trinuclear Complex

In the case of the trinuclear molecule **4** the $\chi_M T$ product of 10.1 cm³ K mol⁻¹ is in the region expected for a complex with three iron(II) centers in the HS state. Upon cooling, a very gradual SCO is observed in the 200 – 125 K temperature region. At 100 K the $\chi_M T$ product of 7.3 cm³ K mol⁻¹ is slightly larger than expected for a trinuclear complex with two HS and one LS iron(II) and in good agreement with the results from single crystal XRD. Upon heating of the sample up to 400 K to remove the methanol molecules included in the crystal packing the SCO behavior is lost and a pure HS species is obtained.

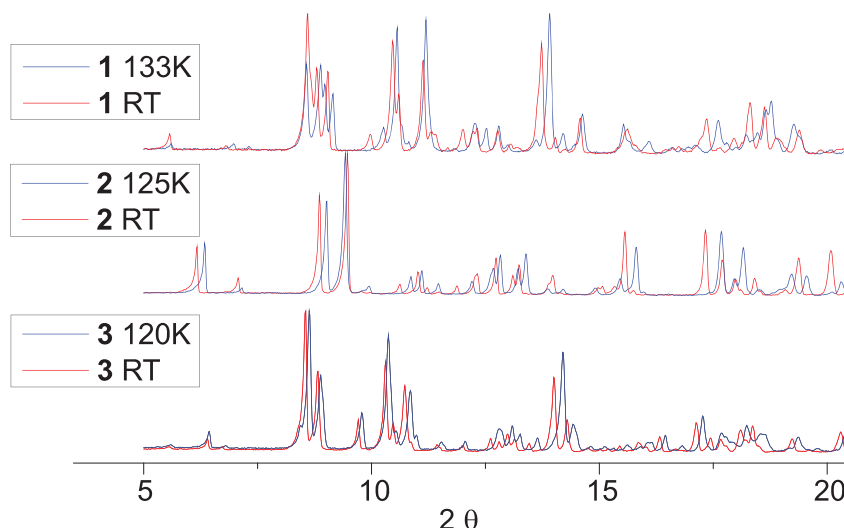


Fig. (4). Powder XRD patterns of the complexes **1** – **3** in the 5 – 20 2θ range.

CONCLUSION

In the manuscript, the synthesis and characterization of five new iron(II) complexes derived from a square-planar templating N_2O_2 ligand platform (L1a/b and L2a/b) in the presence of the urea derivative bpua are presented. The bridging ligand bpua was introduced in order to foster supramolecular communication *via* the formation of interchain hydrogen bond networks; through this cooperative SCO behavior with thermal hysteresis loop should be favored. Four of the complexes are obtained as coordination polymers; this conclusion is substantiated by single-crystal X-ray diffraction of **5** revealing infinite 1-D strands of urea bridged octahedral complex units with HS configuration. Although the crystal structure of **1-3** remains to be determined, we conclude similar topology based upon the results from elemental analysis and the magnetic properties. Compound **5** which derives from ligand L1b is a trinuclear complex consisting of two terminal HS-configured $[Fe(L1b)MeOH]$ units and one central LS-configured $[Fe(L1b)]$ moiety; the overall octahedral coordination spheres are completed by two equivalents of urea bpua, acting as a N_2 -bidentate bridging ligand. Three of the coordination polymers and the trinuclear complex show spin crossover behavior whereas the coordination polymer **4** is a pure HS complex. The results from single crystal XRD indeed show that in both cases hydrogen bond networks are formed. For the complexes **1** and **2** a cooperative ST with hysteresis is observed.

CONSENT FOR PUBLICATION

Not applicable.

CONFLICT OF INTEREST

The authors declare no conflict of interest, financial or otherwise.

ACKNOWLEDGEMENTS

This work was supported financially by the University of Bayreuth.

SUPPLEMENTARY MATERIAL

Supplementary material is available on the publishers web site along with the published article.

REFERENCES

- [1] Catala, L.; Mallah, T. Nanoparticles of Prussian blue analogs and related coordination polymers: From information storage to biomedical applications. *Coord. Chem. Rev.*, **2017**, *346*, 32-61. [<http://dx.doi.org/10.1016/j.ccr.2017.04.005>]
- [2] Ferrando-Soria, J.; Vallejo, J.; Castellano, M.; Martínez-Lillo, J.; Pardo, E.; Cano, J.; Castro, I.; Lloret, F.; Ruiz-García, R.; Julve, M. Molecular magnetism, quo vadis?: A historical perspective from a coordination chemist viewpoint. *Coord. Chem. Rev.*, **2017**, *339*, 17-103. [<http://dx.doi.org/10.1016/j.ccr.2017.03.004>]
- [3] Miller, J.S. Magnetically ordered molecule-based materials. *Chem. Soc. Rev.*, **2011**, *40*(6), 3266-3296. [<http://dx.doi.org/10.1039/c0cs00166j>] [PMID: 21479292]
- [4] Sieklucka, B.; Pinkowicz, D., Eds.; *Molecular Magnetic Materials*; Wiley-VCH Verlag GmbH & Co. KGaA: Weinheim, Germany, **2017**. [<http://dx.doi.org/10.1002/9783527694228>]
- [5] Halcrow, M.A., Ed.; *Spin-Crossover Materials*; John Wiley & Sons Ltd: Chichester, **2013**. [<http://dx.doi.org/10.1002/9781118519301>]
- [6] Gülich, P.; Goodwin, H.A., Eds.; *Spin Crossover in Transition Metal Compounds I-III*; Springer: Berlin / Heidelberg, **2004**.
- [7] Boillot, M.-L.; Weber, B. Mononuclear ferrous and ferric complexes. *C. R. Chim.*, **2018**, *21*, 1196-1208. [<http://dx.doi.org/10.1016/j.crci.2018.01.006>]
- [8] Weber, B.; Bauer, W.; Obel, J. An iron(II) spin-crossover complex with a 70 K wide thermal hysteresis loop. *Angew. Chem. Int. Ed. Engl.*, **2008**, *47*(52), 10098-10101. [<http://dx.doi.org/10.1002/anie.200802806>] [PMID: 19021189]
- [9] Levchenko, G.G.; Bukin, G.V.; Gaspar, A.B.; Real, J.A. The pressure-induced spin transition in the $Fe(phen)_2(NCS)_2$ model compound. *Russ. J. Phys. Chem. A*, **2009**, *83*, 951-954. [<http://dx.doi.org/10.1134/S0036024409060144>]
- [10] Nowak, R.; Prasetyanto, E.A.; De Cola, L.; Bojer, B.; Siegel, R.; Senker, J.; Rössler, E.; Weber, B. Proton-driven coordination-induced spin state switch (PD-CISS) of iron(II) complexes. *Chem. Commun. (Camb.)*, **2017**, *53*(5), 971-974. [<http://dx.doi.org/10.1039/C6CC08618G>] [PMID: 28044155]
- [11] Baldé, C.; Bauer, W.; Kaps, E.; Neville, S.; Desplanches, C.; Chastanet, G.; Weber, B.; Létard, J.F. Light-induced excited spin-state properties in 1D iron(II) chain compounds. *Eur. J. Inorg. Chem.*, **2013**, *2013*, 2744-2750. [<http://dx.doi.org/10.1002/ejic.201201422>]
- [12] Pinkowicz, D.; Rams, M.; Mišek, M.; Kamenev, K.V.; Tomkowiak,

- H.; Katrusiak, A.; Sieklucka, B. Enforcing multifunctionality: A pressure-induced spin-crossover photomagnet. *J. Am. Chem. Soc.*, **2015**, *137*(27), 8795-8802. [http://dx.doi.org/10.1021/jacs.5b04303] [PMID: 26098129]
- [13] Gaspar, A.B.; Weber, B. Spin crossover phenomenon in coordination compounds. *Mole Mag Mater*; Sieklucka, B.; Pinkowicz, D., Eds.; Weinheim, Germany: Wiley-VCH Verlag GmbH & Co. KGaA, **2017**, pp. 231-252. [http://dx.doi.org/10.1002/9783527694228.ch9]
- [14] Feltham, H.L.C.; Bartrop, A.S.; Brooker, S. Spin crossover in iron(II) complexes of 3,4,5-tri-substituted-1,2,4-triazole (Rdpt), 3,5-di-substituted-1,2,4-triazolate (dpt⁻), and related ligands. *Coord. Chem. Rev.*, **2017**, *344*, 26-53. [http://dx.doi.org/10.1016/j.ccr.2016.10.006]
- [15] Ni, Z.-P.; Liu, J.-L.; Hoque, M.N.; Liu, W.; Li, J.-Y.; Chen, Y.-C.; Tong, M.-L. Recent advances in guest effects on spin-crossover behavior in Hofmann-type metal-organic frameworks. *Coord. Chem. Rev.*, **2017**, *335*, 28-43. [http://dx.doi.org/10.1016/j.ccr.2016.12.002]
- [16] Otsubo, K.; Haraguchi, T.; Kitagawa, H. Nanoscale crystalline architectures of Hofmann-type metal-organic frameworks. *Coord. Chem. Rev.*, **2017**, *346*, 123-138. [http://dx.doi.org/10.1016/j.ccr.2017.03.022]
- [17] Senthil Kumar, K.; Ruben, M. Emerging trends in Spin Crossover (SCO) based functional materials and devices. *Coord. Chem. Rev.*, **2017**, *346*, 176-205. [http://dx.doi.org/10.1016/j.ccr.2017.03.024]
- [18] Harding, D.J.; Harding, P.; Phonsri, W. Spin crossover in iron(III) complexes. *Coord. Chem. Rev.*, **2016**, *313*, 38-61. [http://dx.doi.org/10.1016/j.ccr.2016.01.006]
- [19] Brooker, S. Spin crossover with thermal hysteresis: Practicalities and lessons learnt. *Chem. Soc. Rev.*, **2015**, *44*(10), 2880-2892. [http://dx.doi.org/10.1039/C4CS00376D] [PMID: 25907385]
- [20] Gütlich, P.; Gaspar, A.B.; Garcia, Y. Spin state switching in iron coordination compounds. *Beilstein J. Org. Chem.*, **2013**, *9*, 342-391. [http://dx.doi.org/10.3762/bjoc.9.39] [PMID: 23504535]
- [21] Jureschi, C.-M.; Linares, J.; Boulmaali, A.; Dahoo, P.R.; Rotaru, A.; Garcia, Y. Pressure and temperature sensors using two spin crossover materials. *Sensors*, **2016**, *16*, 187/1-187/9. [http://dx.doi.org/10.3390/s16020187]
- [22] Gaspar, A.B.; Seredyuk, M. Spin crossover in soft matter. *Coord. Chem. Rev.*, **2014**, *268*, 41-58. [http://dx.doi.org/10.1016/j.ccr.2014.01.018]
- [23] Luo, Y.H.; Liu, Q.L.; Yang, L.J.; Sun, Y.; Wang, J.W.; You, C.Q.; Sun, B.W. Magnetic observation of above room-temperature spin transition in vesicular nano-spheres. *J. Mater. Chem. C Mater. Opt. Electr. Devices*, **2016**, *4*, 8061-8069. [http://dx.doi.org/10.1039/C6TC02796B]
- [24] Romero-Morcillo, T.; Seredyuk, M.; Muñoz, M.C.; Real, J.A. Melttable spin transition molecular materials with tunable tc and hysteresis loop width. *Angew. Chem. Int. Ed. Engl.*, **2015**, *54*(49), 14777-14781. [http://dx.doi.org/10.1002/anie.201507620] [PMID: 26473403]
- [25] Gandolfi, C.; Morgan, G.G.; Albrecht, M. A magnetic iron(III) switch with controlled and adjustable thermal response for solution processing. *Dalton Trans.*, **2012**, *41*(13), 3726-3730. [http://dx.doi.org/10.1039/c2dt12037b] [PMID: 22366979]
- [26] Garcia, Y.; Su, B.-L.; Komatsu, Y.; Kato, K.; Yamamoto, Y.; Kamihata, H.; Lee, Y.H.; Fuyuhiko, A.; Kawata, S.; Hayami, S. Spin-crossover behaviors based on intermolecular interactions for cobalt(II) complexes with long alkyl chains. *Eur. J. Inorg. Chem.*, **2012**, *2012*, 2769-2775. [http://dx.doi.org/10.1002/ejic.201101040]
- [27] Schlamp, S.; Weber, B.; Naik, A.D.; Garcia, Y. Cooperative spin transition in a lipid layer like system. *Chem. Commun. (Camb.)*, **2011**, *47*(25), 7152-7154. [http://dx.doi.org/10.1039/c1cc12162f] [PMID: 21607245]
- [28] Schlamp, S.; Thoma, P.; Weber, B. Influence of the alkyl chain length on the self-assembly of amphiphilic iron complexes: An analysis of X-ray structures. *Chemistry*, **2014**, *20*(21), 6462-6473. [http://dx.doi.org/10.1002/chem.201304653] [PMID: 24710905]
- [29] Bodenthin, Y.; Schwarz, G.; Tomkowicz, Z.; Lommel, M.; Geue, T.; Haase, W.; Möhwald, H.; Pietsch, U.; Kurth, D.G. Spin-crossover phenomena in extended multi-component metallo-supramolecular assemblies: Deutsche Forschungsgemeinschaft Molecular Magnetism Research Report. *Coord. Chem. Rev.*, **2009**, *253*, 2414-2422. [http://dx.doi.org/10.1016/j.ccr.2008.10.019]
- [30] Gaspar, A.B.; Seredyuk, M.; Gütlich, P. Spin crossover in metallomesogens: Deutsche Forschungsgemeinschaft Molecular Magnetism Research Report. *Coord. Chem. Rev.*, **2009**, *253*, 2399-2413. [http://dx.doi.org/10.1016/j.ccr.2008.11.016]
- [31] Weihermüller, J.; Schlamp, S.; Ditrlich, B.; Weber, B. Kinetic trapping effects in amphiphilic iron(II) spin crossover compounds. *Inorg. Chem.*, **2019**, *58*, 1278-1289. [http://dx.doi.org/10.1021/acs.inorgchem.8b02763] [PMID: 30620576]
- [32] Weihermüller, J.; Schlamp, S.; Milius, W.; Puchler, F.; Breu, J.; Ramming, P.; Hüttner, S.; Agarwal, S.; Göbel, C.; Hund, M.; Papastavrou, G.; Weber, B. Amphiphilic iron(II) spin crossover coordination polymers: Crystal structures and phase transition properties. *J. Mater. Chem. C Mater. Opt. Electr. Devi.*, **2019**, *7*, 1151-1163. [http://dx.doi.org/10.1039/C8TC05580G]
- [33] Zein, S.; Borshch, S.A. Energetics of binuclear spin transition complexes. *J. Am. Chem. Soc.*, **2005**, *127*(46), 16197-16201. [http://dx.doi.org/10.1021/ja054282k] [PMID: 16287309]
- [34] Lochenie, C.; Schötz, K.; Panzer, F.; Kurz, H.; Maier, B.; Puchler, F.; Agarwal, S.; Köhler, A.; Weber, B. Spin-crossover iron(II) coordination polymer with fluorescent properties: Correlation between emission properties and spin state. *J. Am. Chem. Soc.*, **2018**, *140*(2), 700-709. [http://dx.doi.org/10.1021/jacs.7b10571] [PMID: 29251919]
- [35] Kurz, H.; Lochenie, C.; Wagner, K.G.; Schneider, S.; Karg, M.; Weber, B. Synthesis and optical properties of phenanthroline-derived schiff base-like dinuclear Ru^{II}-Ni^{II} complexes. *Chemistry*, **2018**, *24*(20), 5100-5111. [http://dx.doi.org/10.1002/chem.201704632] [PMID: 29143988]
- [36] Schäfer, B.; Bauer, T.; Faus, I.; Wolny, J.A.; Dahms, F.; Fuhr, O.; Lebedkin, S.; Wille, H.-C.; Schlage, K.; Chevalier, K.; Rupp, F.; Diller, R.; Schünemann, V.; Kappes, M.M.; Ruben, M. A luminescent Pt₂Fe spin crossover complex. *Dalton Trans.*, **2017**, *46*(7), 2289-2302. [http://dx.doi.org/10.1039/C6DT04360G] [PMID: 28133662]
- [37] Shepherd, H.J.; Quintero, C.M.; Molnár, G.; Salmon, L.; Bousseksou, A. Luminescent spin-crossover materials. *Spin-Crossover Materials*; Halcrow, M.A., Ed.; John Wiley & Sons Ltd: Chichester, **2013**, pp. 347-373. [http://dx.doi.org/10.1002/9781118519301.ch13]
- [38] Hasegawa, M.; Renz, F.; Hara, T.; Kikuchi, Y.; Fukuda, Y.; Okubo, J.; Hoshi, T.; Linert, W. Fluorescence spectra of Fe(II) spin crossover complexes with 2,6-bis(benzimidazole-2'-yl)pyridine. *Chem. Phys.*, **2002**, *277*, 21-30. [http://dx.doi.org/10.1016/S0301-0104(01)00706-6]
- [39] Faulmann, C.; Jacob, K.; Dorbes, S.; Lampert, S.; Malfant, I.; Doublet, M.-L.; Valade, L.; Real, J.A. Electrical conductivity and spin crossover: A new achievement with a metal bis dithiolene complex. *Inorg. Chem.*, **2007**, *46*(21), 8548-8559. [http://dx.doi.org/10.1021/ic062461c] [PMID: 17850071]
- [40] Dorbes, S.; Valade, L.; Real, J.A.; Faulmann, C. [Fe(sal2-trien)][Ni(dmit)2]: Towards switchable spin crossover molecular conductors. *Chem. Commun. (Camb.)*, **2005**, *(1)*, 69-71. [http://dx.doi.org/10.1039/b412182a] [PMID: 15614375]
- [41] Chen, Y.C.; Meng, Y.; Ni, Z.P.; Tong, M.L. Synergistic electrical bistability in a conductive spin crossover heterostructure. *J. Mater. Chem. C Mater. Opt. Electr. Devi.*, **2015**, *3*, 945-949. [http://dx.doi.org/10.1039/C4TC02580F]
- [42] Ohkoshi, S.; Imoto, K.; Tsunobuchi, Y.; Takano, S.; Tokoro, H. Light-induced spin-crossover magnet. *Nat. Chem.*, **2011**, *3*(7), 564-569. [http://dx.doi.org/10.1038/nchem.1067] [PMID: 21697879]
- [43] Suleimanov, I.; Kraieva, O.; Sánchez Costa, J.; Fritsky, I.O.; Molnár, G.; Salmon, L.; Bousseksou, A. Electronic communication between fluorescent pyrene excimers and spin crossover complexes in nanocomposite particles. *J. Mater. Chem. C Mater. Opt. Electr. Devi.*, **2015**, *3*, 5026-5032. [http://dx.doi.org/10.1039/C5TC00667H]
- [44] Kraieva, O.; Suleimanov, I.; Molnár, G.; Salmon, L.; Bousseksou, A. CdTe quantum dot fluorescence modulation by spin crossover. *Magnetochemistry*, **2016**, *2*, 11. [http://dx.doi.org/10.3390/magnetochemistry2010011]
- [45] Quintero, C.M. Gural'skiy, I'y.A.; Salmon, L.; Molnar, G.; Bergaud, C.; Bousseksou, A. Soft lithographic patterning of spin crossover complexes. Part 1: Fluorescent detection of the spin transition in single nano-objects. *J. Mater. Chem.*, **2012**, *22*, 3745-3751. [http://dx.doi.org/10.1039/c2jm15662h]
- [46] Weber, B. Synthesis of coordination polymer nanoparticles using self-

- assembled block copolymers as template. *Chemistry*, **2017**, *23*(72), 18093-18100.
[<http://dx.doi.org/10.1002/chem.201703280>] [PMID: 28898479]
- [47] Klimm, O.; Göbel, C.; Rosenfeldt, S.; Puchtl, F.; Miyajima, N.; Marquardt, K.; Drechsler, M.; Breu, J.; Förster, S.; Weber, B. Synthesis of $[\text{Fe}(\text{L}(\text{bipy}))_n]$ spin crossover nanoparticles using blockcopolymer micelles. *Nanoscale*, **2016**, *8*(45), 19058-19065.
[<http://dx.doi.org/10.1039/C6NR06330F>] [PMID: 27819367]
- [48] Weber, B.; Bauer, W.; Pfaffeneder, T.; Dítu, M.M.; Naik, A.D.; Rotaru, A.; Garcia, Y. Influence of hydrogen bonding on the hysteresis width in iron(II) spin-crossover complexes. *Eur. J. Inorg. Chem.*, **2011**, *2011*, 3193-3206.
[<http://dx.doi.org/10.1002/ejic.201100394>]
- [49] Lochenie, C.; Bauer, W.; Railliet, A.P.; Schlamp, S.; Garcia, Y.; Weber, B. Large thermal hysteresis for iron(II) spin crossover complexes with N-(pyrid-4-yl)isonicotinamide. *Inorg. Chem.*, **2014**, *53*(21), 11563-11572.
[<http://dx.doi.org/10.1021/ic501624b>] [PMID: 25314334]
- [50] Dankhoff, K.; Lochenie, C.; Puchtl, F.; Weber, B. Solvent influence on the magnetic properties of iron(II) spin-crossover coordination compounds with 4,4'-Dipyridylethine as linker. *Eur. J. Inorg. Chem.*, **2016**, *2016*, 2136-2143.
[<http://dx.doi.org/10.1002/ejic.201501175>]
- [51] Lochenie, C.; Gebauer, A.; Klimm, O.; Puchtl, F.; Weber, B. Iron(ii) spin crossover complexes with diaminoanthalene-based Schiff base-like ligands: 1D coordination polymers. *New J. Chem.*, **2016**, *40*, 4687-4695.
[<http://dx.doi.org/10.1039/C5NJ02470F>]
- [52] Bauer, W.; Lochenie, C.; Weber, B. Synthesis and characterization of 1D iron(II) spin crossover coordination polymers with hysteresis. *Dalton Trans.*, **2014**, *43*(5), 1990-1999.
[<http://dx.doi.org/10.1039/C3DT52635F>] [PMID: 24264535]
- [53] Weber, B. Spin crossover complexes with N_2O_2 coordination sphere-- The influence of covalent linkers on cooperative interactions. *Coord. Chem. Rev.*, **2009**, *253*, 2432-2449.
[<http://dx.doi.org/10.1016/j.ccr.2008.10.002>]
- [54] Weber, B.; Jäger, E-G. Structure and magnetic properties of iron(II/III) complexes with $\text{N}2\text{O}22-$ coordinating schiff base like ligands. *Eur. J. Inorg. Chem.*, **2009**, *2009*, 465-477.
[<http://dx.doi.org/10.1002/ejic.200800891>]
- [55] Baggi, G.; Boiocchi, M.; Fabbrizzi, L.; Mosca, L. Moderate and advanced intramolecular proton transfer in urea-anion hydrogen-bonded complexes. *Chemistry*, **2011**, *17*(34), 9423-9439.
[<http://dx.doi.org/10.1002/chem.201100490>] [PMID: 21732438]
- [56] Becker, H.G.O. *Organikum*, 19th ed; Johann Ambrosius Barth: Berlin, **1993**.
- [57] Lochenie, C.; Heinz, J.; Milius, W.; Weber, B. Iron(II) spin crossover complexes with diaminoanthalene-based Schiff base-like ligands: Mononuclear complexes. *Dalton Trans.*, **2015**, *44*(41), 18065-18077.
[<http://dx.doi.org/10.1039/C5DT03048J>] [PMID: 26415580]
- [58] Thallmair, S.; Bauer, W.; Weber, B. Strategies towards the purposeful design of long-range ferromagnetic ordering due to spin canting. *Polyhedron*, **2009**, *28*, 1796-1801.
[<http://dx.doi.org/10.1016/j.poly.2008.12.010>]
- [59] Lochenie, C.; Bauer, W.; Schlamp, S.; Thoma, P.; Weber, B. Synthesis and characterisation of schiff base-like iron(II) complexes with imidazole as axial ligand. *Z. Anorg. Allg. Chem.*, **2012**, *638*, 98-102.
[<http://dx.doi.org/10.1002/zaac.201100424>]
- [60] Weber, B.; Betz, R.; Bauer, W.; Schlamp, S. Crystal structure of iron(II) acetate. *Z. Anorg. Allg. Chem.*, **2011**, *637*, 102-107.
[<http://dx.doi.org/10.1002/zaac.201000274>]
- [61] Kahn, O. *Molecular Magnetism*; VCH: New York, N.Y., **1993**.
- [62] Burla, M.C.; Caliendo, R.; Camalli, M.; Carrozzini, B.; Cascarano, G.L.; Giacovazzo, C.; Mallamo, M.; Mazzone, A.; Polidori, G.; Spagna, R. SIR2011: A new package for crystal structure determination and refinement. *J. Appl. Cryst.*, **2012**, *45*, 357-361.
[<http://dx.doi.org/10.1107/S0021889812001124>]
- [63] Burla, M.C.; Caliendo, R.; Camalli, M.; Carrozzini, B.; Cascarano, G.L.; de Caro, L.; Giacovazzo, C.; Polidori, G.; Spagna, R. SIR2004: An improved tool for crystal structure determination and refinement. *J. Appl. Cryst.*, **2005**, *38*, 381-388.
[<http://dx.doi.org/10.1107/S002188980403225X>]
- [64] Altomare, A.; Burla, M.C.; Camalli, M.; Cascarano, G.L.; Giacovazzo, C.; Guagliardi, A.; Moliterni, A.G.G.; Polidori, G.; Spagna, R. SIR97: A new tool for crystal structure determination and refinement. *J. Appl. Cryst.*, **1999**, *32*, 115-119.
[<http://dx.doi.org/10.1107/S0021889898007717>]
- [65] Sheldrick, G.M. A short history of SHELX. *Acta Crystallogr. A*, **2008**, *64*(Pt 1), 112-122.
[<http://dx.doi.org/10.1107/S0108767307043930>] [PMID: 18156677]
- [66] Farrugia, L. *WinGX suite for small-molecule single-crystal crystallography*, **1999**, *32*, 837-838.
- [67] Farrugia, L. ORTEP-3 for Windows - a version of ORTEP-III with a Graphical User Interface (GUI). *J. Appl. Cryst.*, **1997**, *30*, 565.
[<http://dx.doi.org/10.1107/S0021889897003117>]
- [68] Johnson, C.K.; Burnett, M.N. *ORTEP-III*; Oak-Ridge, TNOak-Ridge National Laboratory, **1996**.
- [69] Macrae, C.F.; Edgington, P.R.; McCabe, P.; Pidcock, E.; Shields, G.P.; Taylor, R.; Towler, M.; van de Streek, J.; Macrae, C.F.; Edgington, P.R.; McCabe, P.; Pidcock, E.; Shields, G.P.; Taylor, R.; Towler, M.; van de Streek, J. Mercury: Visualization and analysis of crystal structures. *J. Appl. Cryst.*, **2006**, *39*, 453-457.
[<http://dx.doi.org/10.1107/S002188980600731X>]
- [70] Weber, B.; Kaps, E.; Dankhoff, K. Synthesis of a new schiff base-like trinucleating ligand and its copper, vanadyl, and iron complexes - influence of the bridging ligand on the magnetic properties. *Z. Anorg. Allg. Chem.*, **2017**, *643*, 1593-1599.
[<http://dx.doi.org/10.1002/zaac.201700277>]
- [71] Bauer, W.; Weber, B. Magnetism and crystal structure of an N_2O_2 -coordinated iron(II) complex. *Acta Crystallogr. C*, **2008**, *64*(Pt 6), m237-m239.
[<http://dx.doi.org/10.1107/S0108270108013498>] [PMID: 18535332]
- [72] Weber, B.; Kaps, E.; Obel, J.; Bauer, W. Synthesis and magnetic properties of new octahedral iron(II) complexes. *Z. Anorg. Allg. Chem.*, **2008**, *634*, 1421-1426.
[<http://dx.doi.org/10.1002/zaac.200800132>]
- [73] Weber, B.; Obel, J.; Henner-Vasquez, D.; Bauer, W. Two new iron(II) spin-crossover complexes with N_2O_2 coordination sphere and spin transition around room temperature. *Eur. J. Inorg. Chem.*, **2009**, *2009*, 5527-5534.
[<http://dx.doi.org/10.1002/ejic.200900846>]
- [74] Pfaffeneder, T.M.; Thallmair, S.; Bauer, W.; Weber, B. Complete and incomplete spin transitions in 1D chain iron(ii) compounds. *New J. Chem.*, **2011**, *35*, 691-700.
[<http://dx.doi.org/10.1039/C0NJ00750A>]
- [75] Bauer, W.; Pfaffeneder, T.; Achterhold, K.; Weber, B. Complete two-step spin-transition in a 1D chain iron(II) complex with a 110-K wide intermediate plateau. *Eur. J. Inorg. Chem.*, **2011**, *3183*-3192.
[<http://dx.doi.org/10.1002/ejic.201100224>]
- [76] Schlamp, S.; Thoma, P.; Weber, B. New octahedral, head-tail iron(II) complexes with spin crossover properties. *Eur. J. Inorg. Chem.*, **2012**, *2012*, 2759-2768.
[<http://dx.doi.org/10.1002/ejic.201101096>]
- [77] Schönfeld, S.; Lochenie, C.; Thoma, P.; Weber, B. 1D iron(ii) spin crossover coordination polymers with 3,3'-azopyridine - kinetic trapping effects and spin transition above room temperature. *Cryst Eng Comm*, **2015**, *17*, 5389-5395.
[<http://dx.doi.org/10.1039/C5CE00800J>]